A Case for Atmospheric Transmittance: Solar Energy Prediction in Wireless Sensor Nodes

A Case for Atmospheric Transmittance: Solar Energy Prediction in Wireless Sensor Nodes

Stefan Draskovic, Rehan Ahmed, Cong Lin, Lothar Thiele
Computer Engineering and Networks Laboratory, ETH Zurich, Switzerland
Email: {stefan.draskovic, rehan.ahmed, thiele}@tik.ee.ethz.ch, linco@student.ethz.ch

Abstract—In this paper, we propose four novel schemes for solar energy prediction in wireless sensor nodes. Two of the schemes (WCMA-T and ProEnergy-T) are extensions of state-of-the-art schemes, while the remaining schemes (EWMA-T and Delta-T) are new. The proposed strategies leverage the extraterrestrial solar model [5] to get better prediction accuracy compared to state-of-the-art. We restrict our scope to schemes that only employ local information. Thus, leveraging external information, such as weather forecasts, is not permitted. In our comparison, we acknowledge that wireless sensor nodes are resource constrained. In such systems, runtime computation complexity and memory footprint of the prediction schemes is of high importance. Therefore, these overheads are also considered in our comparison. ProEnergy-T achieves an average improvement of 14.5% in accuracy compared to state-of-the-art. Delta-T achieves an average improvement of 8.3% with lower runtime computation complexity.

I. INTRODUCTION

Wireless Sensor Nodes (WSNs) have applications in several application domains such as environmental monitoring [2], [13], surveillance, and automation. Since WSNs are typically deployed in remote locations, they are battery powered. Replenishing the batteries is expensive, and this limitation severely constrains the energy consumption and life-time of WSNs. To alleviate this problem, energy harvesting has been used to prolong the operation of WSNs [6], [3]. This means WSNs harvest energy from the environment to charge their battery. Energy harvesting has been shown to significantly increase the up-time of WSNs, and in the ideal scenario, can achieve perpetual operation; commonly termed energy neutral operation [6]. Under this scenario, the energy consumed by WSNs never exceeds the harvested energy. Also, battery depletion is never encountered and the WSN can run perpetually, assuming that individual system components do not encounter failure.

However, a complication in the design of energy neutral WSNs is the unpredictability of the energy harvesting source. Some of the variations, such as the ones caused by the diurnal solar cycle and the yearly seasons, are deterministic. Other variations, caused by cloud cover or weather, are not deterministic and can, therefore, only be estimated. Several existing works utilize harvestable energy prediction, tightly coupled with power management schemes to achieve energy neutral operation [6], [3], [8]. For such schemes, the prediction accuracy has a high impact on the performance of the WSN, as under-prediction can lead to system under utilization and over-prediction can lead to battery depletion. Therefore, energy neutral WSNs require energy prediction schemes that are both 1) accurate and 2) have low runtime computation and memory overhead. The goal of this paper is to propose such prediction schemes for solar energy, while utilizing only the local history of harvested energy.

Several solar energy prediction schemes exist. Included among them are the Exponentially Weighted Moving Average (EWMA) [6], Weather Conditioned Moving Average (WCMA) [9] and Profile Energy (ProEnergy) [4]. We will overview these schemes in Section II of this paper. In general, all of these schemes leverage the history of harvested energy to predict the energy which will be harvested in the future. Additional schemes also use weather forecasts [10], [11] to improve prediction accuracy. However, we restrict the scope of this paper to schemes where such external sources of information are not exploited, since they may be unavailable or inaccurate for a given deployment location. We improve upon the state-of-the-art by leveraging the extra-terrestrial solar model [5]. Using this model, we can deterministically evaluate the variations in solar energy caused due to diurnal solar cycle and the yearly seasonal variations. Therefore, the schemes proposed in this work try to predict the variation in harvestable solar energy caused solely by transiently changing factors such as weather. This leads to an improved prediction accuracy, characterized here using the Mean Absolute Percentage Error (MAPE). The following four schemes are proposed:

1) **WCMA-T**: An extension of WCMA [9]. Has a prediction accuracy as good as the existing schemes (average MAPE = 23.39) with the computation and memory overhead slightly higher than WCMA.
2) **ProEnergy-T**: An extension of ProEnergy [4]. Improves the precision of ProEnergy at the cost of a small additional computation and memory overhead. ProEnergy-T has best prediction accuracy (average MAPE = 20.97) among the existing and new schemes.
3) **EWMA-T**: A new prediction scheme that achieves high accuracy (average MAPE = 22.68) with very low computation and memory overhead.
4) **Delta-T**: A new prediction scheme that achieves high accuracy (average MAPE = 22.21) with very low computation and memory overhead. Computation and memory overhead of Delta-T is higher compared to EWMA-T.

This paper is organized as follows: Section II covers state-of-the-art solar energy prediction schemes. Section III covers

the proposed energy prediction algorithms. We summarize the extra-terrestrial solar model in this section and evaluate the runtime complexity of the proposed and existing schemes. The proposed and existing schemes are evaluated in Section IV followed by the conclusion and appendix.

II. RELATED RESEARCH

A plethora of solar energy prediction algorithms exist. However, in this paper we will focus only on ones suitable for WSNs. Before introducing related research in this domain, we introduce some important notation which is used to both explain related work and present the new energy prediction schemes.

Firstly, we assume that each day is discretized into 24 one-hour, 12 two-hour or 6 four-hour time-slots. This resolution was found to be commonly used for WSNs [6]. Secondly, energy harvested by an ideal $1\,\mathrm{m}^2$ solar panel placed horizontally, on day d at time-slot t (or between times $t-1$ and t), shall be denoted by $E_{d,t}$. $\widehat{E}_{d,t}$ will denote the *predicted* energy harvested for the same day and time-interval.

The first scheme, Exponentially Weighted Moving Average (EWMA) [6] prediction is simple yet widely used. As its name suggests, it predicts energy $\widehat{E}_{d,t}$ as an exponentially weighted moving average[1] of energy harvested in the same time-slot in the previous days. EWMA can be computed recursively using:

$$\widehat{E}_{d,t} = \alpha \cdot \widehat{E}_{d-1,t} + (1 - \alpha) \cdot E_{d-1,t} \qquad (1)$$

where α is a weighting factor between 0 and 1. The advantages of EWMA are clear as the scheme is very easy to implement, and it is effective when there are no major day-to-day weather changes. The main disadvantage is a high error when there are changing weather conditions; for example when sunny and cloudy days are alternating.

Another scheme better suited for alternating weather is Weather-Conditioned Moving Average (WCMA) [9]. This scheme observes the average energy harvested at a given hour in the past D days, and introduces a scaling factor GAP_k that quantifies how the current day's weather is with respect to the average. The scaling factor is then used to make a prediction using:

$$\widehat{E}_{d,t} = \alpha \cdot E_{d,t-1} + GAP_k \cdot (1 - \alpha) \cdot \frac{1}{D} \cdot \sum_{i=d-1}^{d-D} E_{i,t} \qquad (2)$$

WCMA responds to a weather change after one time-slot, while EWMA needs a full day to take this change into account. Therefore, it is expected that the former scheme is more suitable for frequently changing weather conditions. This comes at a cost though, which is the computation time needed to derive the GAP_k factor, where k is a parameter that denotes the number of time-slots used for calculating the factor (see [9] for details).

A third approach, introduced in [4], is the Profile Energy Prediction model (ProEnergy). Instead of utilizing certain average values as in the former schemes, ProEnergy takes a different approach by keeping D full days of observed energy harvesting traces, called profiles. Ideally, these D profiles are chosen as representatives of different weather conditions encountered. Thus, to make a prediction, we need to find the most similar day among the memorized D profiles. If p_d is this similar profile, and α is a weighting factor[2], the predicted energy can be computed using (3).

$$\widehat{E}_{d,t} = \alpha \cdot E_{d,t-1} + (1 - \alpha) \cdot E_{p_d,t} \qquad (3)$$

Practically speaking, ProEnergy involves building and possibly updating the D representative profile list, then finding the most similar profile, and finally calculating the predicted value. By taking advantage of a representative list of profiles, ProEnergy promises to outperform both WCMA and EWMA. The drawback is a larger computation and memory footprint needed to run the scheme.

Additional schemes which use weather forecasts to improve prediction accuracy have also been proposed [10], [11]. However, these schemes are excluded from the comparison presented in this work. The reason for exclusion is two fold: 1) weather forecast data may be unavailable or inaccurate for a given location, and 2) when accurate forecast data is available, its effect on the prediction accuracy of the proposed schemes is expected to be complementary, since such forecast will improve error caused by weather changes. The schemes proposed in this paper are still of value, since they reduce error caused by diurnal solar cycle and yearly season changes.

To our knowledge, atmospheric transmittance has been used by two research works [3], [1] for solar energy prediction. In [3], Buchli et al. use extraterrestrial model based solar energy predictor to design a power management scheme with the objective of long-term operation of the WSN. However, [3] focuses on long prediction intervals (one week) as opposed to short term predictions (one to four hours) which are the focus of this paper. Therefore, the approach in [3] is not directly applicable. In [1], Bao et al. use the extraterrestrial model along with externally acquired cloud cover information to predict energy. Because of the externally sourced information, it is not directly applicable in our scenario.

We conclude with an *ideal* prediction scheme, which predicts harvested energy in the next interval perfectly, while consuming only nominal computation time and memory space.

III. SOLAR ENERGY PREDICTION

In this section we present the proposed solar energy prediction schemes. We first overview the extraterrestrial solar model. Following this, we propose solar energy prediction schemes that leverage the extraterrestrial solar model to yield significantly better prediction accuracy compared to state-of-the-art with low computation and memory overhead.

A. Extraterrestrial model

Determining the position of the Sun in the sky is a well studied phenomenon [5]. Using the Sun's position, we can

---

[1]The contribution of old data to the average is exponentially decreasing.

[2]In the original work, for medium-term energy predictions the weighting factor can be a function of the similarity of days d and p_d.

θ^{lat}	Latitude in radians. North values positive
θ^{lon}	Longitude in radians. East values positive
ε_d	Eccentricity correction factor of Earth's orbit on day d
Γ_d	Day angle on day d in radians
I	Constant rate of extraterrestrial energy $= 1353 Wm^{-2}$
δ_d	Solar declination angle on day d
EoT_d	Equation of time on day d
time_zone	Time zone of a location with out day light saving.
$\mathrm{AST}_{d,t}$	Apparent solar time at day d and time t
$\omega_{d,t}$	Solar angle at day d and time t
ω_d^{sr}	Solar angle at sunrise on day d
$\theta_{d,t}^z$	Solar zenith angle at day d and time t

Fig. 1. Histogram of RSD of atmospheric transmittance and solar energy, within a given day

deterministically calculate the energy harvested by a $1\,\mathrm{m}^2$ solar panel above the atmosphere; commonly called the extraterrestrial irradiation model.

For our analysis and evaluations, it is assumed that the solar panel is oriented horizontally, tangent to the Earth's surface. However, extending to arbitrary orientations is trivially possible. $E_{d,t}^{\mathrm{et}}$ is used to denote energy harvested by a $1\,\mathrm{m}^2$ horizontally oriented solar panel in the interval $(t-1, t]$ of day d. Table I defines all the parameters and terms that are needed to compute $E_{d,t}^{\mathrm{et}}$. For detailed explanation of these parameters, please refer to [5]. The equations used for computing the terms from the table are given in Appendix A. The appendix also states the equations needed to compute the solar irradiation model for arbitrarily oriented surfaces in Appendix A1.

B. Atmospheric transmittance and its utility

In this section, we define atmospheric transmittance and explain how it can be computed and used to design energy prediction schemes. The average atmospheric transmittance during time interval t of day d is the ratio between the energy harvested during time interval t of day d, and the extraterrestrial energy harvested during the same interval:

$$S_{d,t} = E_{d,t}/E_{d,t}^{\mathrm{et}} \qquad (4)$$

The predicted value of atmospheric transmittance is analogously given below. Note that the extraterrestrial energy in the equation is not a predicted value, as the extraterrestrial energy of every interval is known.

$$\widehat{S}_{d,t} = \widehat{E}_{d,t}/E_{d,t}^{\mathrm{et}} \qquad (5)$$

Predicting $\widehat{S}_{d,t}$ and using it to compute the value of $\widehat{E}_{d,t}$ is expected to improve prediction accuracy over existing prediction schemes. This is because $E_{d,t}^{\mathrm{et}}$ accurately models the diurnal solar cycle and the yearly seasonal variations. Therefore, any error caused by *predicting* these deterministic variations will be removed. To illustrate this advantage, we show the histogram of the Relative Standard Deviation (RSD) of atmospheric transmittance and solar energy within a given day[3]. RSD is a measure of relative variation in a data. As seen

[3]Data taken from the NSRDB [12] Seattle WA site. Values less than 10% of the given day's maximum value were omitted for RSD computation.
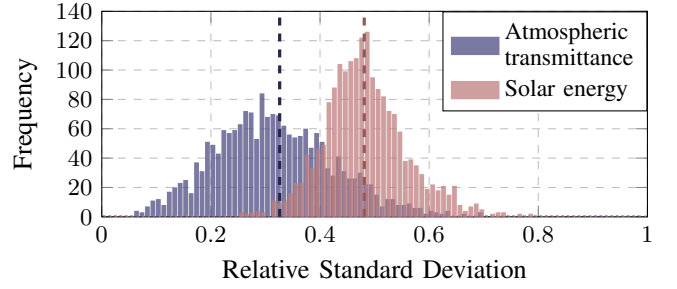
in Fig. 1, the RSD of atmospheric transmittance has a lower mean value compared to the corresponding metric for solar energy. This is precisely because considering atmospheric transmittance removes variations caused by the diurnal solar cycle. Therefore, the prediction error in transmittance based schemes is expected to be less compared to the existing schemes, which work directly on high variance solar energy.

C. Transmittance based prediction models

Here we propose four transmittance based prediction schemes. Weather Conditioned Moving Average - Transmittance (WCMA-T) and Profile Energy - Transmittance (ProEnergy-T) are simple enhancements of state-of-the-art schemes, while Exponentially Weighted Moving Average - Transmittance (EWMA-T) and Delta - Transmittance (Delta-T) are novel.

1) Enhancing existing schemes: Let us demonstrate how transmittance is used to predict energy by explaining ProEnergy-T. First, transmittance can not be directly measured, but has to be computed from the observed harvested energy using (4). Next, with the transmittance at time $t-1$ in place, as well as D transmittance profiles memorized, we may predict the transmittance at time t using:

$$\widehat{S}_{d,t} = \alpha \cdot S_{d,t-1} + (1-\alpha) \cdot S_{p_d,t} \qquad (6)$$

Finally by applying (5) we obtain a predicted harvested energy value. WCMA-T is defined in a similar manner, where (6) is replaced by the following equation:

$$\widehat{S}_{d,t} = \alpha \cdot S_{d,t-1} + GAP_k \cdot (1-\alpha) \cdot \frac{1}{D} \cdot \sum_{i=d-1}^{d-D} S_{i,t} \qquad (7)$$

Computationally, both schemes have the added overhead of computing the transmittance.

2) EWMA-T: The idea behind Exponentially Weighted Moving Average - Transmittance (EWMA-T) is that transmittance does not change abruptly within a given day. Therefore it can be predicted as the exponentially weighted moving average of previous hours. It is thus defined as:

$$\widehat{S}_{d,t} = \alpha \cdot \widehat{S}_{d,t-1} + (1-\alpha) \cdot S_{d,t-1} \qquad (8)$$

This scheme promises to combine the benefit of predicting transmittance with the simplicity of EWMA.

TABLE II
COMPUTATION COSTS

Scheme	Computations per execution		Additional daily comp.
EWMA	(1)	$3C_S$	—
WCMA	(2)	$7C_S$	—
	GAP_k	$2k{\cdot}C_S+C_A$	
ProEnergy	(3)	$3C_S$	—
	finding p_d	$6D{\cdot}C_S$	
transmittance overhead	(4) and (5)	C_S+C_A	—
	$E_{d,t}^{\mathrm{et}}$	$11C_S+2C_A$	$42C_S+7C_A$
WCMA-T	Same as WCMA		
ProEnergy-T	Same as ProEnergy		
EWMA-T	(8)	$3C_S$	—
Delta-T	(9)	$3C_S+C_A$	—

TABLE III
MEMORY COSTS

Scheme	Variables to be stored between executions	Size
EWMA	Predicted energy for next T time-slots	T
WCMA	Observed energy of last D days	$D \cdot T$
	Carry over values	$k+T$
ProEnergy	Observed energy of chosen D days	$D \cdot T$
	Last T observed energy values	T
	Carry over values	D
transmittance overhead	Daily and hourly parameters	16
WCMA-T	Same as WCMA	
ProEnergy-T	Same as ProEnergy	
EWMA-T	Predicted transmittance for next time-slot	1
Delta-T	Observed transmittance of last D days	$D \cdot T$
	Carry over values	T

TABLE IV
EVALUATED LOCATIONS

Location	Site ID	lat	lon	TZ	Climate
Adak AK (ADAK)	704540	51.53	-176.39	-10	Cfc
Barrow AK (BARR)	700260	71.19	-156.37	-9	ET
Fargo ND (FARG)	727530	46.56	-96.49	-6	Dfb
Honolulu HI (HONO)	911820	21.19	-157.56	-10	As
New York NY (NYC)	744860	40.39	-73.48	-5	Cfa
Phoenix AZ (PHEX)	722780	33.27	-111.59	-7	Bwh
Seattle WA (SEAT)	727930	47.28	-122.19	-8	Csb

3) Delta-T: The intuition behind Delta-Transmittance (Delta-T) is that the change in transmittance from time-slot $t-1$ to time-slot t follows a similar pattern across the last D days. Therefore, the prediction can be formulated as:

$$\widehat{S}_{d,t} = S_{d,t-1} \cdot \frac{\sum_{i=d-1}^{d-D} S_{i,t}}{\sum_{i=d-1}^{d-D} S_{i,t-1}} \tag{9}$$

Because of the need to store $D \cdot t$ transmittance values, and to compute the associated sums, Delta-T requires more resources than EWMA-T. The actual comparison of runtime complexity is done in the following section.

D. Computation and memory cost

In this section, we revisit all of the aforementioned schemes in order to compare their computation and memory costs. First, we present Table II where the number of computations for all of the schemes are compared. In the table, C_S denotes an operation that is either addition, subtraction or multiplication, while C_A denotes division or a trigonometric function. For transmittance based schemes, the cost for calculating the current extraterrestrial energy $E_{d,t}^{\mathrm{et}}$, as well as the cost of calculating transmittance from energy and vice versa, has *not* been included in the computational cost, but given separately as 'transmittance overhead'. Note that for ProEnergy and ProEnergy-T, the number of computations needed for a profile update is not given.

Table III displays memory cost, i.e. the variables that need to be stored between two consecutive executions. While presenting the memory cost, T denotes the number of daylight hours per day.

IV. RESULTS

In this section, we first introduce metrics used to evaluate data, then the dataset, and finally we evaluate all of the aforementioned schemes.

A. Metrics

To evaluate the precision of all mentioned schemes, two metrics are used: Mean Absolute Error (MAE) and Mean Absolute Percentage Error (MAPE). They can be computed using:

$$\mathrm{MAE} = \frac{1}{N} \sum_{i=1}^{N} \left| \widehat{E_i} - E_i \right| \tag{10}$$

$$\mathrm{MAPE} = 100 \cdot \frac{1}{N} \sum_{i=1}^{N} \left| 1 - \frac{\widehat{E_i}}{E_i} \right| \tag{11}$$

MAPE is usually used by related work to show the relative accuracy of a prediction scheme. However, we note that a relative measure might not be sufficient to give a complete overview of a scheme's performance; most notably MAPE gives little information when harvested energy is close to zero. We therefore introduce MAE, which comments on the absolute accuracy of the prediction scheme, to supplement our evaluation. Note that some papers use an alternative formula for MAPE, where $\frac{E_i}{\widehat{E_i}}$ is used instead of $\frac{\widehat{E_i}}{E_i}$. While evaluating both metrics, night time and low light time-slots are omitted unless otherwise noted – these are defined to be time-slots in which the energy harvested is less than 10% of the daily maximum. This practice is common in related work (i.e. [9], [4]). We also provide results for prediction accuracy for each hour individually, and in these results the low light time-slots are not ignored.

B. Dataset

Evaluations were performed on the National Solar Radiation Database (NSRDB) [12]. From this database, meteorologically diverse sites given in Table IV were selected. The latitude,
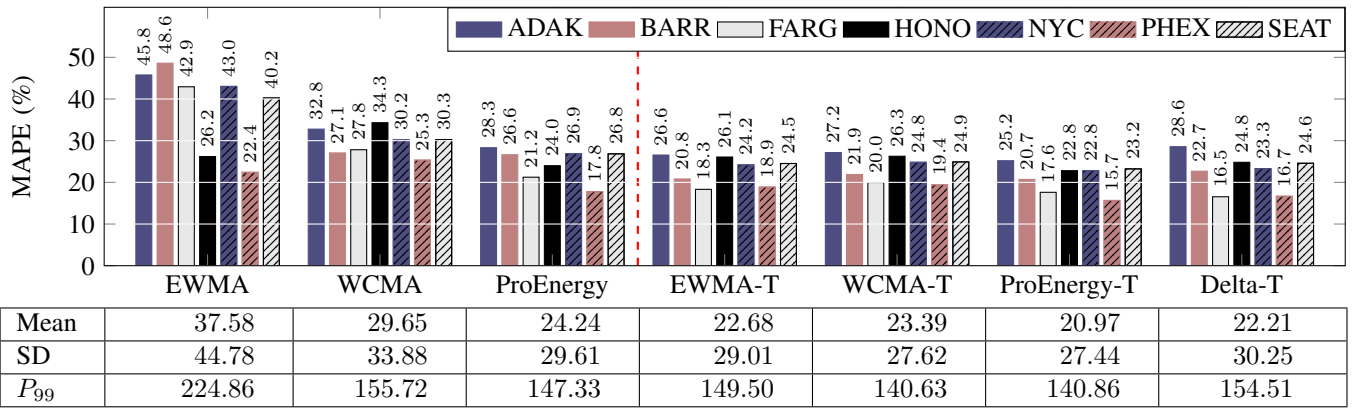
	EWMA	WCMA	ProEnergy	EWMA-T	WCMA-T	ProEnergy-T	Delta-T
Mean	37.58	29.65	24.24	22.68	23.39	20.97	22.21
SD	44.78	33.88	29.61	29.01	27.62	27.44	30.25
P_{99}	224.86	155.72	147.33	149.50	140.63	140.86	154.51

Fig. 2. Mean Absolute Percentage Error in solar energy prediction for existing and proposed schemes

	EWMA	WCMA	ProEnergy	EWMA-T	WCMA-T	ProEnergy-T	Delta-T
Mean	104.41	85.02	71.60	69.90	71.11	63.88	69.63
SD	99.83	85.86	77.50	83.43	79.31	75.48	85.42
P_{99}	443.48	388.22	360.01	391.05	373.22	354.10	395.20
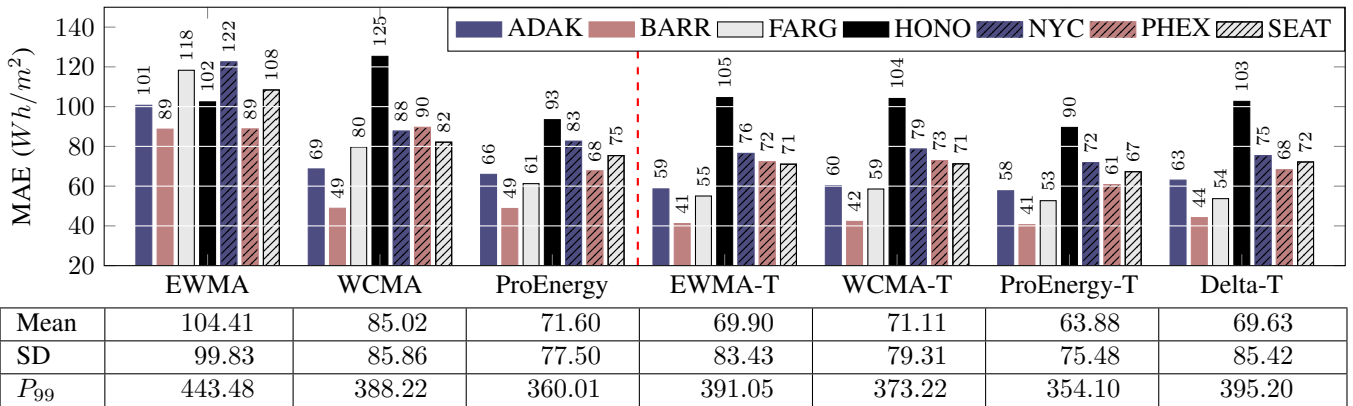
Fig. 3. Mean Absolute Error in solar energy prediction for existing and proposed schemes

longitude and time-zone values given in Table IV were used to calculate atmospheric transmittance for the proposed schemes. The Köppen Climate Classification subtype [7] of all locations is also given in Table IV to highlight their meteorological diversity. Data was collected from years 2005-2009. Year 2005 data was used for training, i.e. for each individual scheme, parameters which gave the minimum error[4] were found. These parameters are: weighting factor α for EWMA and EWMA-T; weighting factor α, number of past days D, and k parameter for WCMA and WCMA-T; weighting factor α and number of stored days D for ProEnergy and ProEnergy-T; and number of past days D for Delta-T. In addition, for updating profiles in ProEnergy and ProEnergy-T, three other parameters are optimized: maximal age, number of combined profiles, and β; see [4] for details. These parameters were then fixed and evaluation was conducted on the remaining four years.

C. Evaluation

Four types of evaluation are used to characterize the schemes. First, we show how schemes compare at different locations. Then, for one location, we compute the metrics at different times of day, and for different prediction interval

[4]Separate training was conducted for MAPE and MAE.

lengths. Finally, we end the section with a MAPE versus computation complexity analysis.

a) Location: The performance of all of the schemes, on the seven evaluation locations, is given in Figures 2 and 3. These figures show the MAPE and MAE for every scheme and location, as well as the mean, standard deviation (SD), and 99-percentile (P_{99}) value for all locations together.

What we can observe first is that EWMA is, w.r.t. MAPE, the least precise scheme overall, as well as for individual locations – except Honolulu HI and Phoenix AZ where it outperforms WCMA. For all other locations, WCMA is more precise than EWMA. Regardless of the metric and location, ProEnergy performes best of the non-transmittance based schemes.

Out of the transmittance based schemes w.r.t. MAPE, the best scheme overall is ProEnergy-T, having the best precision for all evaluated locations except Fargo ND. WCMA-T has the least precision and performs arguably as good as ProEnergy (e.g. performing worse than it in Phoenix AZ, and better than it in Seattle WA). EWMA-T and Delta-T both perform slightly better than WCMA-T, though the exact amount depends on the actual location (e.g. for Fargo ND Delta-T is better, followed by EWMA-T and WCMA-T, while for Adak AK it is EWMA-T followed by WCMA-T and Delta-T).

The results for MAE are similar to MAPE. However, we
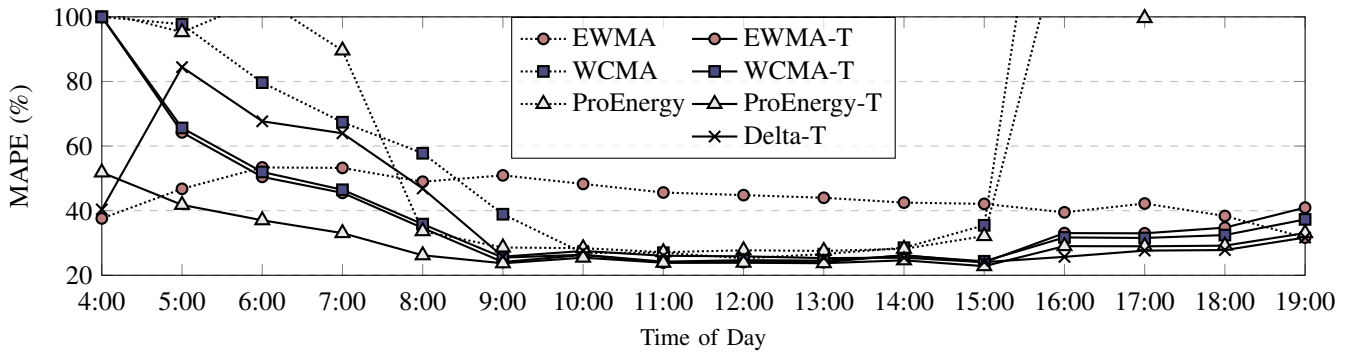
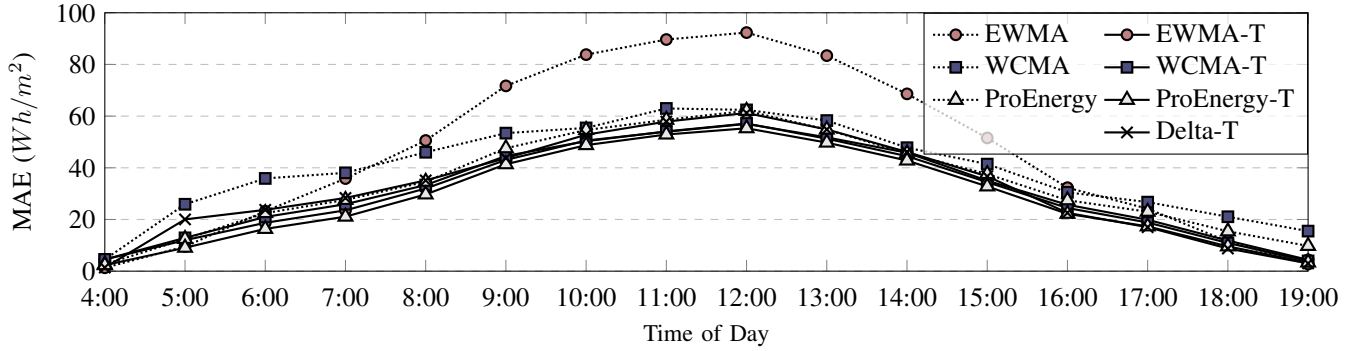Fig. 4. MAPE for Seattle WA, for each daylight hour

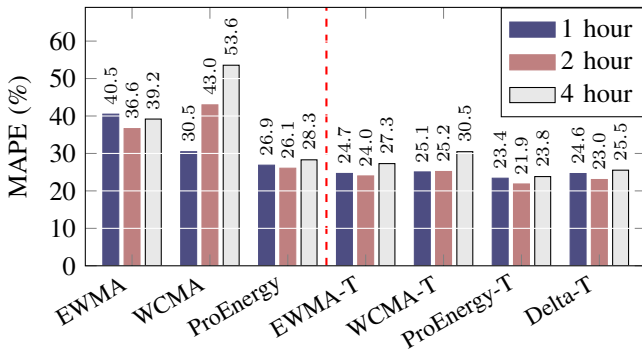Fig. 5. MAE for Seattle WA, for each daylight hour

Fig. 6. MAPE for Seattle WA, for one, two and four hour prediction intervals
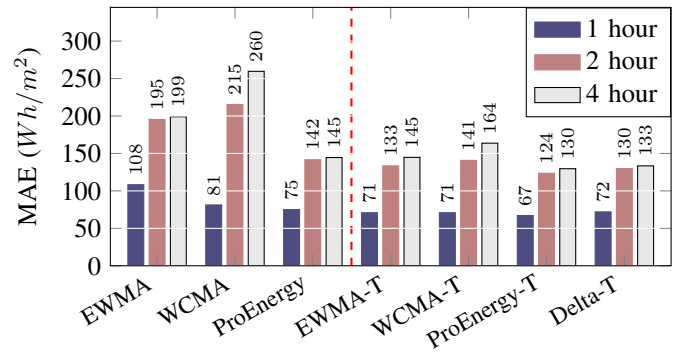

Fig. 7. MAE for Seattle WA, for one, two and four hour prediction intervals

see the effect of the amount of harvestable solar energy. On the one side, Honolulu HI has a lot of sunshine so the absolute error is high for most of the schemes, even though the relative one is not. On the other side, Barrow AK is located inside the Arctic Circle, thus the absolute error for all of the schemes is low.

b) Time of Day: To supplement the evaluation at different locations, the performance of all the schemes is evaluated independently for different times of day. Figures 4 and 5 show the MAPE and MAE for every scheme, at location Seattle WA, averaged for each hour of a day. Here, every data point with positive harvested energy has been taken into account.

With regards to MAPE, all schemes perform the worst in the early morning hours, up to 8 o'clock. The exception is

EWMA, as its precision is roughly the same throughout the day. Nevertheless, ProEnergy-T has the best performance in the morning, arguably followed by EWMA-T and WCMA-T. Considering the midday hours, ProEnergy-T has the best performance here as well, and the other transmittance based schemes slightly outperform non-transmittance based schemes. During afternoon and evening hours, after 15 o'clock, transmittance based schemes improve prediction accuracy considerably. The four transmittance based schemes perform similarly, with Delta-T preforming best.

The results for MAE complement the above observations, by showing that the absolute errors in prediction are low in the morning and evening, and high during midday.
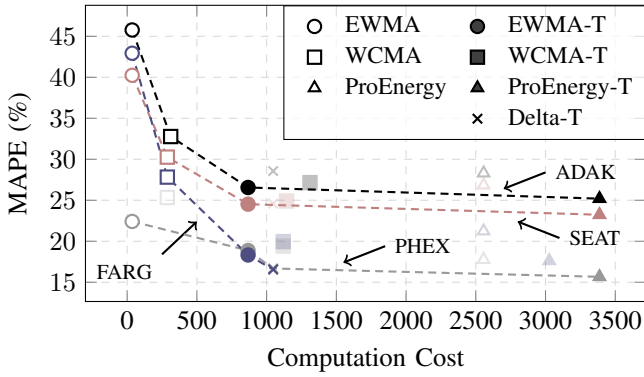
Fig. 8. Pareto plot showing the MAPE and computation complexity of existing and proposed schemes. Not included is the cost for updating profiles for ProEnergy and ProEnergy-T

c) Prediction interval length: The effect of the prediction interval length on the MAPE and MAE is evaluated next. Figures 6 and 7 show the performance of every scheme for one, two and four hour intervals, at location Seattle WA. The MAPE varies little in each scheme, except for WCMA which is less precise for longer prediction intervals. The MAE, however, is roughly double when two or four hour prediction intervals are used, as opposed to one hour intervals. This is primarily because more energy is harvested in larger intervals, though due to the diurnal cycle the increase is not linear.

d) Complexity: To give complexity measures, we assume that complex floating point operations (trigonometric operations and their inverse, division) take 15 time units and basic arithmetic operations (addition, subtraction, multiplication) take 1 time unit. Fig. 8 plots the MAPE and the computation cost for predicting twelve one-hour time-slots in a single day. Fig. 8 presents results for all schemes and for four different geographical locations. In the figure, all schemes that are Pareto dominated for a given location are *dimmed*. The Pareto fronts for all locations are illustrated by dashed lines. Note that some schemes do not have the same computation cost on all locations, as location-dependent optimization parameters impact this cost. Fig. 8 shows that EWMA has minimum computation cost for all locations. However, it has significantly high MAPE compared to the other schemes, with the exception of location Phoenix AZ. It should be noted that the new transmittance based schemes (EWMA-T, Delta-T) have better MAPE than the most accurate existing scheme (ProEnergy), and a reduced computation cost, for all locations. ProEnergy-T is the most accurate scheme, with the exception of Fargo ND, where Delta-T outperforms ProEnergy-T. However, the accuracy of Delta-T and EWMA-T is comparable to the accuracy of ProEnergy-T, with significantly lower computation cost. It should be noted that the computation cost for the transmittance based schemes can be significantly lowered if the $E_{d,t}^{\text{et}}$ is stored on the WSN for the entire year. This would result in a memory cost $24 \times 365 = 8760$ read-only floating point numbers, which is feasible on many modern embedded platforms.

V. Conclusion

In this paper, we present new mechanisms for predicting solar energy that exploit the extraterrestrial solar model [5]. Using this model results in significant improvement in prediction accuracy (ProEnergy-T yields 14.5% improvement in MAPE compared to existing schemes), with a small additional computation cost (about 800 additional computations performed in a single day). We also propose computationally less expensive prediction schemes (EWMA-T, Delta-T) that provide comparable prediction accuracy with lower computation cost.

References

[1] Y. Bao, X. Wang, X. Liu, S. Zhou, and Z. Niu. Solar radiation prediction and energy allocation for energy harvesting base stations. In *Communications (ICC), 2014 IEEE International Conference on*, pages 3487–3492. IEEE, 2014.

[2] J. Beutel, B. Buchli, F. Ferrari, M. Keller, and M. Zimmerling. X-sense: Sensing in extreme environments. In *Design, Automation & Test in Europe Conference & Exhibition (DATE), 2011*, pages 1–6. IEEE, 2011.

[3] B. Buchli, F. Sutton, J. Beutel, and L. Thiele. Dynamic power management for long-term energy neutral operation of solar energy harvesting systems. In *Proceedings of the 12th ACM Conference on Embedded Network Sensor Systems*, pages 31–45. ACM, 2014.

[4] A. Cammarano, C. Petrioli, and D. Spenza. Pro-energy: A novel energy prediction model for solar and wind energy-harvesting wireless sensor networks. In *Mobile Adhoc and Sensor Systems (MASS), 2012 IEEE 9th International Conference on*, pages 75–83, 2012.

[5] M. Iqbal. *An introduction to solar radiation*. Elsevier, 2012.

[6] A. Kansal, J. Hsu, S. Zahedi, and M. B. Srivastava. Power management in energy harvesting sensor networks. *ACM Transactions on Embedded Computing Systems (TECS)*, 6(4):32, 2007.

[7] W. Köppen and R. Geiger. *Handbuch der klimatologie*, volume 3. Gebrüder Borntraeger Berlin, Germany, 1930.

[8] C. Moser, D. Brunelli, L. Thiele, and L. Benini. Real-time scheduling for energy harvesting sensor nodes. *Real-Time Systems*, 37(3):233–260, 2007.

[9] J. R. Piorno, C. Bergonzini, D. Atienza, and T. S. Rosing. Prediction and management in energy harvested wireless sensor nodes. In *Wireless Communication, Vehicular Technology, Information Theory and Aerospace & Electronic Systems Technology, 2009. Wireless VITAE 2009. 1st International Conference on*, pages 6–10, 2009.

[10] N. Sharma, J. Gummeson, D. Irwin, and P. Shenoy. Cloudy computing: Leveraging weather forecasts in energy harvesting sensor systems. In *Sensor Mesh and Ad Hoc Communications and Networks (SECON), 2010 7th Annual IEEE Communications Society Conference on*, pages 1–9. IEEE, 2010.

[11] N. Sharma, P. Sharma, D. Irwin, and P. Shenoy. Predicting solar generation from weather forecasts using machine learning. In *Smart Grid Communications (SmartGridComm), 2011 IEEE International Conference on*, pages 528–533. IEEE, 2011.

[12] S. Wilcox. National solar radiation database 1991-2010 update: User's manual. Technical report, National Renewable Energy Laboratory (NREL), Golden, CO., 2010.

[13] P. Zhang, C. M. Sadler, S. A. Lyon, and M. Martonosi. Hardware design experiences in zebranet. In *Proceedings of the 2nd international conference on Embedded networked sensor systems*, pages 227–238. ACM, 2004.

Appendix

A. Extraterrestrial Model Equations

$$\Gamma_d = 2\pi(d-1)/365 \tag{12}$$

$$\begin{aligned}
\varepsilon_d = &\, 1.00011 + 0.034221\cos(\Gamma_d) \\
&+ 0.00128\sin(\Gamma_d) + 0.000719\cos(2\Gamma_d) \\
&+ 0.000077\sin(2\Gamma_d)
\end{aligned} \tag{13}$$

Daily changing parameters	
Γ_d	C_S
$\text{Cos}(\Gamma_d), \text{Sin}(\Gamma_d), \text{Cos}(\delta_d), \text{Sin}(\delta_d)$	C_A
$\text{Cos}(2\Gamma_d), \text{Sin}(2\Gamma_d), \text{Cos}(3\Gamma_d), \text{Sin}(3\Gamma_d)$	$3C_S$
$I \cdot \varepsilon_d \cdot 12/\pi$	$8C_S$
δ_d	$12C_S$
$\text{EoT}_d/60 + 4(\theta^{\text{lon}} - 15\ \text{time\_zone})/60$	$8C_S$
ω_d^{sr}	$3C_A + C_S$
Hourly changing parameters	
$\text{AST}_{d,t}$	C_S
$\omega_{d,t}$	$2C_S$
$E_{d,t}^{\text{et}}$	$8C_S + 2C_A$

$\theta_{d,t}^a$	Solar azimuth angle at day d time t
β	Slope of the surface measured from horizontal
γ	Azimuth angle of the surface
$\theta_{d,t}$	Solar incidence angle on the inclined surface at day d time t
$\omega_d^{\text{sr*}}$	Sunrise solar angle for the inclined surface on day d
$\omega_d^{\text{ss*}}$	Sunset solar angle for the inclined surface on day d

$$\delta_d = 0.006918 - 0.399912\cos(\Gamma_d)$$
$$+ 0.070257\sin(\Gamma_d) - 0.006758\cos(2\Gamma_d)$$
$$+ 0.000907\sin(2\Gamma_d) - 0.002697\cos(3\Gamma_d) \quad (14)$$
$$+ 0.00148\sin(3\Gamma_d)$$

$$\text{EoT}_d = 229.18\big(0.000075 + 0.001868\cos(\Gamma_d)$$
$$- 0.032077\sin(\Gamma_d) - 0.04089\sin(2\Gamma_d) \quad (15)$$
$$- 0.014615\cos(2\Gamma_d)\big)$$

$$\text{AST}_{d,t} = t + \frac{\text{EoT}_d + 4(\theta^{\text{lon}} - 15\ \text{time\_zone})}{60} \quad (16)$$

$$\omega_{d,t} = 15(12 - \text{AST}_{d,t}) \quad (17)$$
$$\omega_d^{\text{sr}} = \cos^{-1}\big(-\tan(\delta_d) \cdot \tan(\theta^{\text{lat}})\big) \quad (18)$$
$$\theta_{d,t}^z = \cos^{-1}\big(\cos(\delta_d) \cdot \cos(\theta^{\text{lat}}) \cdot \cos(\omega_{d,t})$$
$$+ \sin(\delta_d) \cdot \sin(\theta^{\text{lat}})\big) \quad (19)$$

Assuming that sunrise or sunset does not occur during a given time-slot x, we can use the following equation to compute the extraterrestrial energy on a horizontal surface:

$$E_{d,x}^{\text{et}} = I \cdot \varepsilon_d \cdot \int_{x-1}^{x} \cos(\theta_{d,t}^z)\, dt$$

In general, the following equation can be used:

$$E_{d,t}^{\text{et}} = I \cdot \varepsilon_d \cdot 12/\pi \Big(\sin(\delta_d) \cdot \sin(\theta^{\text{lat}})\big(\omega_{d,t-1}^* - \omega_{d,t}^*\big)$$
$$+ \cos(\delta_d) \cdot \cos(\theta^{\text{lat}})\big(\sin(\omega_{d,t-1}^*) - \sin(\omega_{d,t}^*)\big)\Big) \quad (20)$$

where $\omega_{d,t}^*$ is given by:

$$\omega_{d,t}^* = \begin{cases} \min(\omega_{d,t}, \omega_d^{\text{sr}}) & \text{If } \omega_{d,t} \geq 0 \\ \max(\omega_{d,t}, -\omega_d^{\text{sr}}) & \text{If } \omega_{d,t} < 0 \end{cases}$$

Table V presents the computation cost of the extraterrestrial solar model. Computations required to evaluate $E_{d,t}^{\text{et}}$ for one day, assuming 12 hours of daylight are: $174C_S + 31C_A$.

1) Computing extraterrestrial irradiation for arbitrarily oriented surfaces: Please refer to Section 1.6 of [5] for a detailed explanation of equations/parameters presented in this section. For an arbitrarily oriented solar panel, we define the additional terms presented in Table VI.

$$\theta_{d,t}^a = \cos^{-1}\left(\frac{\cos(\theta_{d,t}^z) \cdot \sin(\theta^{\text{lat}}) - \sin(\delta_d))}{\sin(\theta_{d,t}^z) \cdot \cos(\theta^{\text{lat}})}\right) \quad (21)$$

$$\theta_{d,t} = \cos^{-1}\Big(\cos(\beta) \cdot \cos(\theta_{d,t}^z)$$
$$+ \sin(\beta) \cdot \sin(\theta_{d,t}^z) \cdot \cos(\theta_{d,t}^a - \gamma)\Big) \quad (22)$$

Using the incidence angle, we can compute extraterrestrial irradiation using the following equation:

$$E_{d,t}^{\text{et}} = I \cdot \varepsilon_d \cdot \int_{x-1}^{x} \cos(\theta_{d,t})\, dt \quad (23)$$

For computation of incidence angle in (23), the solar angles need to adjusted based on the sunrise and sunset angles, in the following manner:

$$\omega_{d,t}^* = \begin{cases} \max(\omega_{d,t}, \omega_d^{\text{sr*}}) & \text{If } \omega_{d,t} \geq 0 \\ \max(\omega_{d,t}, \omega_d^{\text{ss*}}) & \text{If } \omega_{d,t} < 0 \end{cases}$$

The sunrise and setset angle will differ depending on the orientation of the surface. For a surface, oriented towards the east, we have the following equations:

$$\omega_d^{\text{sr*}} = \min\left\{\omega_d^{\text{sr}}, \cos^{-1}\left(\frac{-x \cdot y - \sqrt{x^2 - y^2 + 1}}{x^2 + 1}\right)\right\} \quad (24)$$

$$\omega_d^{\text{ss*}} = -\min\left\{\omega_d^{\text{sr}}, \cos^{-1}\left(\frac{-x \cdot y + \sqrt{x^2 - y^2 + 1}}{x^2 + 1}\right)\right\} \quad (25)$$

For a surface oriented towards the west, we have the following equations:

$$\omega_d^{\text{sr*}} = \min\left\{\omega_d^{\text{sr}}, \cos^{-1}\left(\frac{-x \cdot y + \sqrt{x^2 - y^2 + 1}}{x^2 + 1}\right)\right\} \quad (26)$$

$$\omega_d^{\text{ss*}} = -\min\left\{\omega_d^{\text{sr}}, \cos^{-1}\left(\frac{-x \cdot y - \sqrt{x^2 - y^2 + 1}}{x^2 + 1}\right)\right\} \quad (27)$$

where:

$$x = \frac{\cos(\theta^{\text{lat}})}{\sin(\gamma) \cdot \tan(\beta)} + \frac{\sin(\theta^{\text{lat}})}{\tan(\gamma)} \quad (28)$$

$$y = \tan(\delta_d)\left(\frac{\sin(\theta^{\text{lat}})}{\sin(\gamma) \cdot \tan(\beta)} - \frac{\cos(\theta^{\text{lat}})}{\tan(\gamma)}\right) \quad (29)$$